supra, Results Section A) brings on competition between the amino donor atoms of the NCN′ system and the PR_3 ligands for binding to the Ni(II) center. Only with $((t\text{-Bu})MeNCN')^-$ can two types of complexes, i.e. $[NiBr((t\text{-Bu})MeNCN')]$ (**5**) and $[NiBr((t\text{-Bu})MeNCN')(PR_3)_2]$ (**7**) be synthesized; the former is accessible via routes A and C (see Experimental Section). We have not been able to synthesize $[NiBr((Ph)MeNCN')]$, in which the $((Ph)MeNCN')^-$ ligand would be bonded in the terdentate mode. Looking at the yields of the syntheses, it seems that in the complexes $[NiBr(R^1R^2NCN')]$ the nitrogen donor atoms become poorer ligands in the order R^1 = Me, *i*-Pr, *t*-Bu (R^2 = Me). This trend is confirmed by the values of the Ni-N distances which become larger in the order $[Ni(O_2CH)(Me_2NCN')]$,[7] $[NiBr((i\text{-Pr})MeNCN')]$, $[NiBr((t\text{-Bu})MeNCN')]$ (vide supra, Results Section C). From these data the following decreasing ligand strength order toward Ni(II) can be given for the R^1R^2N donor atoms:

$$Me_2N > Et_2N > (i\text{-Pr})MeN > (t\text{-Bu})MeN > (Ph)MeN$$

The place of $i\text{-Pr}_2N$ is difficult to give. $[NiBr(i\text{-Pr}_2NCN')]$ (**3**) could only be isolated via route C in poor yields (vide supra), but that is not a good criterion for the ligand strength of the $i\text{-Pr}_2NCH_2$- unit. The reactions of $(i\text{-Pr}_2NCN'Li)_n$ (made in situ) with $[NiBr_2(PEt_3)_2]$ and $i\text{-Pr}_2NCN'Br$ with $[Ni(COD)_2]$ are probably hampered by the steric hindrance of the reaction sites by the four large *i*-Pr groups. This ligand strength order of the R^1R^2N groups toward Ni(II) is not the same as that for the ligand strength of various R^1R^2N groups toward Pt(II), which was found to be decreasing in the order $Me_2N \sim (t\text{-Bu})MeN > Et_2N > (Ph)MeN > Ph_2N$.[16]

Acknowledgment. Prof. K. Vrieze is kindly thanked for his stimulating interest in this research. The Netherland Foundation for Chemical Research (SON) and the Netherland Organization for Scientific Research (NWO) are thanked for financial support (J.A.M.vB., W.J.J.S., and A.L.S.). X-ray data for **8b** were collected by A. J. M. Duisenberg.

Supplementary Material Available: For the structure determinations of **4b**, **5**, and **8b**, tables of crystal data, anisotropic thermal parameters, hydrogen atom parameters, and bond distances and angles, indicating torsion angles for **8b** (13 pages); tables listing observed and calculated structure factors (50 pages). Ordering information is given on any current masthead page.

Contribution from the Department of Chemistry and Molecular Structure Center, Indiana University, Bloomington, Indiana 47405

Incorporation of Barium for the Synthesis of Heterometallic Alkoxides: Synthesis and Structures of $[BaZr_2(O^iPr)_{10}]_2$ and $Ba\{Zr_2(O^iPr)_9\}_2$

Brian A. Vaarstra, John C. Huffman, William E. Streib, and Kenneth G. Caulton*

Received January 15, 1991

Barium granules and barium hexamethyldisilazide tetrahydrofuranate are used as reagents for the introduction of barium in the syntheses of heterometallic zirconium isopropoxides. Reaction with 1 or 2 equiv of $Zr_2(O^iPr)_8(HO^iPr)_2$ yields $[BaZr_2(O^iPr)_{10}]_2$ and $Ba\{Zr_2(O^iPr)_9\}_2$, respectively. The structure of the former has been determined in the solid state by X-ray diffraction studies. Crystal data (-78 °C): a = 18.066 (3) Å, b = 12.549 (2) Å, c = 19.409 (3) Å, β = 94.42° with Z = 2 in the space group $P2_1/c$. The structure reveals a dimer in which all metal centers are six-coordinate. The compound is also characterized by ^1H and ^{13}C NMR spectroscopy and elemental analysis. X-ray diffraction data for $Ba\{Zr_2(O^iPr)_9\}_2$ are not acceptably refined but indicate gross skeletal features in which barium is eight-coordinate, surrounded by two $Zr_2(O^iPr)_9^-$ fragments.

Introduction

Metal alkoxides are of interest in ceramics processing technology and are used in the production of oxide monometallic materials by methods such as the sol-gel process.[1] While mixtures of alkoxides have been extensively used, heterometallic alkoxides are attractive precursors to *multi*metallic oxide materials due to a potentially fixed and homogeneous control over the desired metal stoichiometry on the molecular level.[2] It is also possible that desired structural features can be carried on from the precursor to the oxide lattice.

In order to demonstrate the utility of heterometallic alkoxides as precursors to solid-state oxide materials, synthetic strategy for control of a desired metal stoichiometry must be developed. We have recently demonstrated that the proton of an alcohol adduct of a metal alkoxide provides a manipulable functional group by which to incorporate additional metal ions.[3-5]

In this paper, redox and acid-base chemistry are employed in order to incorporate barium into a zirconium isopropoxide "matrix" via the alcoholate dimer $Zr_2(O^iPr)_8(HO^iPr)_2$. The particular interest in barium arises from its occurrence in a number of high-T_c superconducting oxides, such as $YBa_2Cu_3O_7$, and the present work with zirconium serves as a testing ground for our synthetic procedure for rational linking of distinct metallic elements.

Experimental Section

All manipulations were carried out under helium or argon in a drybox and with Schlenk techniques. All solvents were dried and distilled prior to use and stored under argon. Barium granules were purchased from Alfa Products, and $Zr_2(O^iPr)_8(HO^iPr)_2$ was obtained from Aldrich Chemical Co. The compound $Ba\{N(SiMe_3)_2\}_2(THF)_2$ was made by the previously reported procedure.[6] Infrared spectra were recorded on a Nicolet 510P FTIR spectrometer as Nujol mulls between KBr plates. NMR spectra were obtained on a Bruker AM500 instrument, with chemical shifts referenced to solvent resonances. Elemental analyses were provided by Oneida Research Services, Whitesboro, NY.

Syntheses. Method 1. For either $[BaZr_2(O^iPr)_{10}]_2$ (**1**) or $Ba\{Zr_2(O^iPr)_9\}_2$ (**2**), the appropriate amounts of $Zr_2(O^iPr)_8(HO^iPr)_2$ (0.496 and 0.576 g, respectively) and Ba granules (0.088 and 0.051 g) were loaded into a Schlenk tube. After the addition of 5 mL of THF, the zirconium isopropoxide dissolved and the solution was heated to reflux in order to activate the barium metal surface. Evolution of H_2 began after a few minutes, and the solution was then allowed to stir for 24 h at 25 °C. After this time, all of the Ba metal had disappeared, although there was an insoluble precipitate in the solution. The solution was stripped to dryness in vacuo, and the product was redissolved in pentane. The mixture was filtered, and the product was recrystallized from cold pentane. Both products are colorless, crystalline solids.

Method 2. For either $[BaZr_2(O^iPr)_{10}]_2$ (**1**) or $Ba\{Zr_2(O^iPr)_9\}_2$ (**2**), the appropriate amount of $Ba\{N(SiMe_3)_2\}_2(THF)_2$ (0.155 and 0.078 g, re-

(1) *Sol-Gel Technology for Thin Films, Fibers, Preforms, Electronics and Specialty Shapes*; Klein, L. C., Ed.; Noyes Publications: Park Ridge, NJ, 1988.
(2) (a) Hubert-Pfalzgraf, L. G. *New. J. Chem.* **1987**, *11*, 663. (b) Caulton, K. C.; Hubert-Pfalzgraf, L. G. *Chem. Rev.* **1990**, *90*, 969.
(3) Vaartstra, B. A.; Huffman, J. C.; Streib, W. E.; Caulton, K. G. *J. Chem. Soc., Chem. Commun.* **1990**, 1750.
(4) Vaartstra, B. A.; Huffman, J. C.; Gradeff, P. S.; Hubert-Pfalzgraf, L. G.; Daran, J.-C.; Parraud, S.; Yunlu, K.; Caulton, K. G. *Inorg. Chem.* **1990**, *29*, 3126.
(5) Vaartstra, B. A.; Streib, W. E.; Caulton, K. G. *J. Am. Chem. Soc.* **1990**, *112*, 8593.
(6) Vaartstra, B. A.; Huffman, J. C.; Streib, W. E.; Caulton, K. G. *Inorg. Chem.* **1991**, *30*, 121.

0020-1669/91/1330-3068$02.50/0

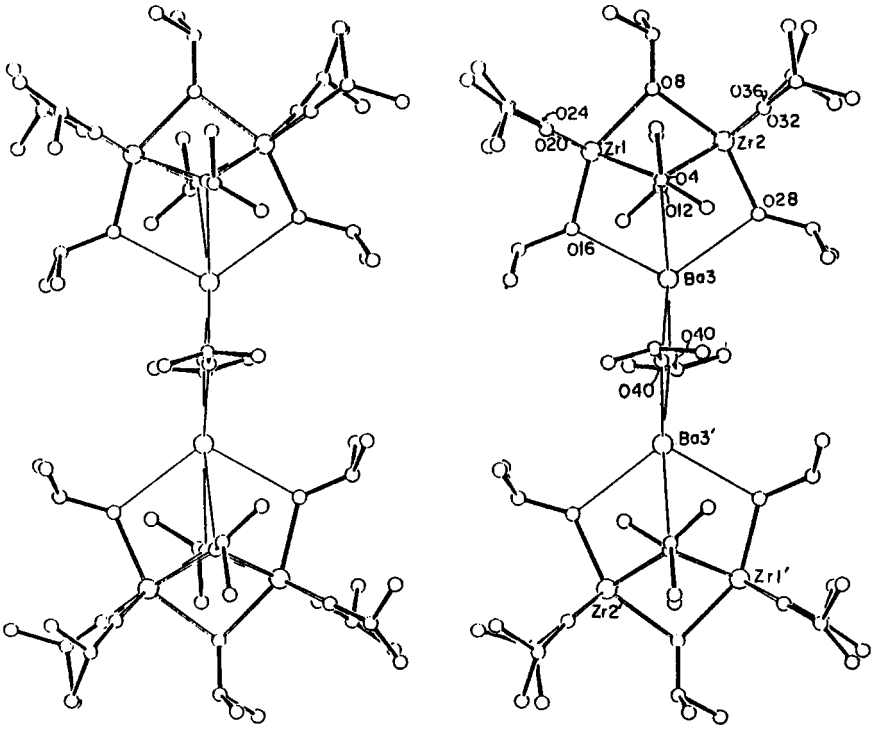

Figure 1. Stereo ORTEP drawing of the non-hydrogen atoms of $[BaZr_2(O^iPr)_{10}]_2$, showing selected atom labeling. A crystallographic center of symmetry lies between Ba(3) and Ba(3)' and generates the lower (primed) half of the molecule from the upper half.

spectively) was weighed out and dissolved in 10 mL of pentane. For **1**, a solution of 0.200 g for $Zr_2(O^iPr)_8(HO^iPr)_2$ in 10 mL pentane was slowly added to the $Ba\{N(SiMe_3)_2\}_2(THF)_2$ solution via cannula transfer. The solution was stirred for 30 min and then heated to reflux for several minutes. For **2**, the solution of $Ba\{N(SiMe_3)_2\}_2(THF)_2$ was slowly added to a solution of 0.200 g of $Zr_2(O^iPr)_8(HO^iPr)_2$ in 10 mL pentane, which had been cooled to 0 °C. The solution was stirred for 17 h at 0 °C. Each solution was then filtered and stripped to dryness in vacuo. Extra precaution was taken with **2**, keeping it at or below temperature. The NMR spectra of the resulting white solids indicated good sample purity with yields above 90% in each case. Crystallization from cold pentane further improves purity (for analysis, melting point), but their solubility in pentane drastically reduces the yield of recrystallized material.

$[BaZr_2(O^iPr)_{10}]_2$ (1). ^1H NMR (toluene-d_8): δ 4.68 (sept, 2 H), 4.59 (sept, 2 H), 4.56 (sept, 1 H), 4.51 (sept, 4 H), 4.24 (sept, 1 H), 1.68 (d, 12 H), 1.46 (d, 6 H), 1.43 (d, 6 H), 1.42 (d, 12 H), 1.38 (d, 12 H), 1.36 (d, 12 H). $^{13}C\{^1H\}$ NMR (toluene-d_8): δ 71.44, 70.03, 69.31, 68.69, 64.02, (*CH*, int = 4:1:2:2:1); δ 30.65, 28.17, 27.45, 27.33 (*CH*$_3$; see text). Infrared (cm^{-1}): 1192 (m), 1175 (vs), 1144 (vs), 1128 (vs), 1022 (st), 1011 (st), 968 (vs), 947 (m), 847 (m), 831 (m), 820 (m). Anal. Calcd for $BaZr_2O_{10}C_{30}H_{70}$: C, 39.57; H, 7.75. Found: C, 39.18; H, 7.51. Mp: 278–280 °C.

$Ba\{Zr_2(O^iPr)_9\}_2$ (2). ^1H NMR (toluene-d_8): δ 4.60 (sept, 1 H), 1.52 (d, 6 H). $^{13}C\{^1H\}$ NMR (toluene-d_8): δ 70.22, 27.58. ^1H NMR (toluene-d_8, −60 °C): δ 4.69 (partially resolved septet), 4.59 (mult, int = 1:2); δ 1.75, 1.71, 1.60, 1.59, 1.44, 1.42 (unstructured, int = 2:3:2:5:2:2). Infrared (cm^{-1}): 1186 (m), 1173 (v), 1130 (vs), 1019 (s), 1005 (s), 963 (s), 945 (m), 845 (m), 829 (m), 820 (m). Anal. Calcd for $BaZr_4O_{18}C_{54}H_{126}$: C, 41.42, H, 8.11. Found: C, 40.91; H, 7.85. Mp: 154–156 °C dec.

Alcohol-free $[Zr(O^iPr)_4]_n$, shown by Bradley and Holloway[7] to have an average of $n = 3.57$, was obtained by heating $Zr_2(O^iPr)_8(^iPrOH)_2$ in vacuum at 150 °C for 4 h. ^1H NMR (25 °C, C_6D_6): δ 1.43 (d, 6 H), 4.61 (sept, 1 H).

X-ray Structure Determination of $[BaZr_2(O^iPr)_{10}]_2$. A suitable crystal was located and transferred to the goniostat by using standard inert-atmosphere handling techniques and cooled at −78 °C for characterization and data collection.[8] Initial examination of crystals at −145 °C indicated a catastrophic phase transition, and the study reported here was performed at a temperature just above that observed for the transition. A systematic search of a limited hemisphere of reciprocal space located a set of diffraction maxima with symmetry and systematic absences corresponding to the unique monoclinic space group $P2_1/c$. Subsequent solution and refinement of the structure confirmed this choice.

Table I. Crystallographic Data for $[BaZr_2(O^iPr)_{10}]_2$

chem formula	$C_{60}H_{140}O_{20}Ba_2Zr_4$	space group	$P2_1/c$
a, Å	18.066 (3)	T, °C	−78
b, Å	12.549 (2)	λ, Å	0.71069
c, Å	19.409 (3)	ρ_{calcd}, g cm^{-3}	1.379
β, deg	94.42 (0)	μ(Mo Kα), cm^{-1}	13.87
V, Å^3	4386.88	$R(F)$	0.0611
Z	2	$R_w(F)$	0.0600
fw	1821.31		

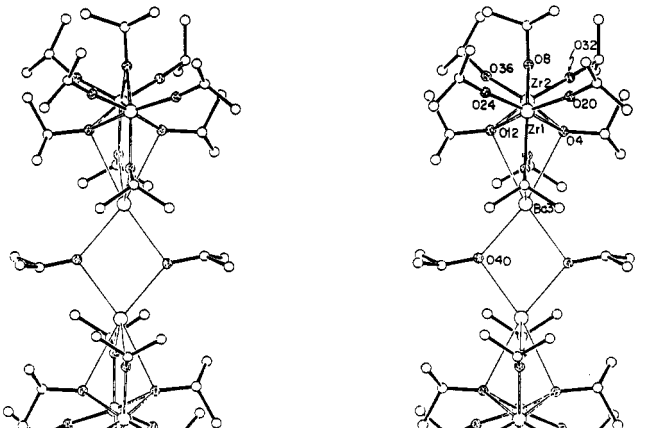

Figure 2. Stereo ORTEP drawing of $[BaZr_2(O^iPr)_{10}]_2$, rotated 90° from Figure 1. Oxygen atoms are stippled.

Data were collected ($6° \le 2\theta \le 45°$) in the usual manner[8] by using a continuous θ–2θ scan with fixed backgrounds. Parameters of the unit cell and the data collection are given in Table I. Data were reduced to a unique set of intensities and associated σ's in the usual manner. Difficulty was encountered in phasing by using standard direct-methods techniques (MULTAN78). *E*-maps consistently yielded the barium and one zirconium, with numerous other false peaks. Once the second Zr was located, solution proceeded smoothly. A slight disorder occurs in two of the isopropyl groups, and alternate positions are given for atoms C(7) and

(7) Bradley, D. C.; Holloway, C. E. *J. Chem. Soc. A* **1968**, 1316.
(8) Huffman, J. C.; Lewis, L. N.; Caulton, K. G. *Inorg. Chem.* **1990**, *19*, 2755.

Table II. Fractional Coordinates and Isotropic Thermal Parameters[a] for $[BaZr_2(O^iPr)_{10}]_2$

	10^4x	10^4y	10^4z	$10B_{iso}$, Å^2
Zr(1)	7836 (1)	9586 (1)	1384 (1)	38
Zr(2)	7683 (1)	12148 (1)	1045.4 (5)	34
Ba(3)	6011.5 (3)	10435 (1)	448.6 (3)	36
O(4)	7062 (3)	10917 (5)	1609 (3)	33
C(5)	6725 (7)	11097 (12)	2243 (5)	58
C(6)	7277 (8)	11315 (13)	2837 (6)	78
C(7)	6151 (8)	11886 (14)	2207 (8)	50
O(8)	8503 (3)	11041 (5)	1546 (3)	40
C(9)	9236 (6)	11273 (10)	1809 (7)	58
C(10)	9788 (6)	10981 (14)	1303 (9)	84
C(11)	9404 (9)	10676 (17)	2484 (9)	103
O(12)	7596 (3)	10635 (5)	453 (3)	33
C(13)	7818 (7)	10423 (12)	-237 (6)	60
C(14)	8644 (8)	10486 (14)	-272 (7)	79
C(15)	7541 (16)	9557 (23)	-562 (13)	67
O(16)	6881 (4)	8841 (5)	995 (3)	43
C(17)	6721 (7)	7730 (11)	1035 (8)	65
C(18)	6073 (10)	7579 (14)	1449 (9)	100
C(19)	6581 (12)	7263 (15)	328 (10)	116
O(20)	7895 (4)	9013 (6)	2308 (4)	57
C(21)	8037 (11)	8498 (17)	2955 (9)	115
C(22)	8597 (15)	7793 (23)	3029 (10)	180
C(23)	7349 (14)	8261 (22)	3266 (12)	167
O(24)	8561 (4)	8691 (6)	985 (4)	59
C(25)	9100 (10)	7977 (15)	779 (10)	105
C(26)	9603 (13)	7616 (21)	1276 (11)	160
C(27)	8823 (11)	7290 (17)	228 (13)	134
O(28)	6657 (4)	12452 (5)	552 (4)	45
C(29)	6326 (8)	13433 (12)	347 (8)	72
C(30)	5646 (16)	13681 (24)	680 (16)	196
C(31)	6163 (20)	13465 (25)	-387 (11)	220
O(32)	7704 (4)	13225 (5)	1764 (4)	47
C(33)	7750 (8)	14071 (11)	2253 (7)	67
C(34)	8518 (9)	14169 (15)	2566 (9)	94
C(35)	7432 (13)	15050 (14)	1933 (10)	119
O(36)	8328 (4)	12860 (6)	449 (4)	56
C(37)	8879 (10)	13466 (13)	142 (8)	86
C(38)	9342 (9)	14081 (15)	652 (10)	100
C(39)	8550 (13)	14089 (19)	-436 (10)	145
O(40)	5353 (4)	9906 (6)	-711 (3)	47
C(41)	5467 (12)	9829 (19)	-1388 (9)	120
C(42)	5795 (10)	8822 (21)	-1582 (10)	134
C(43)	5698 (13)	10727 (24)	-1782 (10)	146
C(7)′	6161 (27)	10386 (41)	2438 (25)	81 (9)
C(15)′	7405 (14)	11163 (21)	-773 (13)	62 (6)

[a] Isotropic values for those atoms refined anisotropically are calculated by using the formula given by: Hamilton, W. C. *Acta Crystallogr.* **1959**, *12*, 609.

C(15). Refinement of occupancies indicated that C(7) is closer to a 70:30 ratio, while C(15) is 50:50. The ORTEP drawings reflect only one position for each. Idealized hydrogen positions (d_{CH} = 0.95 Å) were used in the final refinement. As seen in the figures, the molecule possesses a crystallographic center of inversion. A final difference Fourier was featureless, with the largest peak being 0.84 e/Å^3. The results of the structure determination are shown in Tables II and III and Figures 1 and 2.

Results

Syntheses, Spectral Data, and Thermal Stability. The reaction of barium granules with either 1 or 2 equiv of $Zr_2(O^iPr)_8(HO^iPr)_2$ proceeds at ambient temperature over 24 h after an initial heating to activate the Ba surfaces. While this method forms the compounds $[BaZr_2(O^iPr)_{10}]_2$ (**1**) and $Ba\{Zr_2(O^iPr)_9\}_2$ (**2**), using 1 and 2 equiv of $Zr_2(O^iPr)_8(HO^iPr)_2$, respectively, it is difficult to prohibit contamination of **1** by **2** and vice versa.

In order to better control the reaction stoichiometry and product purity, the recently reported[6] soluble monomeric barium species $Ba[N(SiMe_3)_2]_2(THF)_2$ was employed. Slow addition of a pentane solution of the barium hexamethyldisilazide to a pentane solution of $Zr_2(O^iPr)_8(HO^iPr)_2$ should favor formation of **2** over **1** and the reverse order of addition should favor formation of **1**. Coupled with control of the desired Ba:Zr mole ratio for each product, this method reduces the contamination of one by the other to less than 10% as determined by NMR spectroscopy. Further, it was found that **2** thermally decomposes to **1** quite readily (see below) and synthesis of **2** at lower temperatures is therefore helpful.

Table III. Selected Bond Distances (Å) and Angles (deg) for $[BaZr_2(O^iPr)_{10}]_2$

Ba(3)–O(4)	2.895 (6)	Zr(1)–O(16)	2.054 (7)
Ba(3)–O(12)	2.873 (6)	Zr(1)–O(20)	1.926 (7)
Ba(3)–O(16)	2.709 (7)	Zr(1)–O(24)	1.932 (7)
Ba(3)–O(28)	2.787 (7)	Zr(2)–O(4)	2.243 (6)
Ba(3)–O(40)	2.551 (7)	Zr(2)–O(8)	2.202 (6)
Ba(3)–O(40)′	2.592 (7)	Zr(2)–O(12)	2.219 (6)
Zr(1)–O(4)	2.243 (6)	Zr(2)–O(28)	2.055 (7)
Zr(1)–O(8)	2.196 (7)	Zr(2)–O(32)	1.940 (7)
Zr(1)–O(12)	2.252 (6)	Zr(2)–O(36)	1.924 (7)
O(4)–Ba(3)–O(12)	52.17 (16)	O(4)–Zr(2)–O(28)	83.56 (25)
O(4)–Ba(3)–O(16)	61.58 (19)	O(4)–Zr(2)–O(32)	96.43 (26)
O(4)–Ba(3)–O(28)	60.58 (18)	O(4)–Zr(2)–O(36)	164.2 (3)
O(4)–Ba(3)–O(40)	166.86 (19)	O(8)–Zr(2)–O(12)	72.99 (23)
O(4)–Ba(3)–O(40)′	117.25 (19)	O(8)–Zr(2)–O(28)	151.03 (26)
O(12)–Ba(3)–O(16)	61.04 (19)	O(8)–Zr(2)–O(32)	98.48 (27)
O(12)–Ba(3)–O(28)	60.62 (19)	O(8)–Zr(2)–O(36)	98.1 (3)
O(12)–Ba(3)–O(40)	114.93 (18)	O(12)–Zr(2)–O(28)	83.81 (25)
O(12)–Ba(3)–O(40)′	167.63 (19)	O(12)–Zr(2)–O(32)	164.87 (26)
O(16)–Ba(3)–O(28)	114.55 (19)	O(12)–Zr(2)–O(36)	96.2 (3)
O(16)–Ba(3)–O(40)	111.72 (22)	O(28)–Zr(2)–O(32)	99.9 (3)
O(16)–Ba(3)–O(40)′	109.45 (23)	O(28)–Zr(2)–O(36)	101.5 (3)
O(28)–Ba(3)–O(40)	117.63 (23)	O(32)–Zr(2)–O(36)	97.4 (3)
O(28)–Ba(3)–O(40)′	122.33 (23)	Zr(1)–O(4)–Zr(2)	94.26 (22)
O(40)–Ba(3)–O(40)′	75.22 (23)	Zr(1)–O(4)–C(5)	126.7 (7)
O(4)–Zr(1)–O(8)	72.37 (22)	Zr(2)–O(4)–C(5)	124.9 (7)
O(4)–Zr(1)–O(12)	68.71 (22)	Zr(1)–O(8)–Zr(2)	96.77 (23)
O(4)–Zr(1)–O(16)	83.79 (24)	Zr(1)–O(8)–C(9)	135.4 (7)
O(4)–Zr(1)–O(20)	95.0 (3)	Zr(2)–O(8)–C(9)	127.6 (7)
O(4)–Zr(1)–O(24)	164.4 (3)	Zr(1)–O(12)–Zr(2)	94.70 (21)
O(8)–Zr(1)–O(12)	72.46 (22)	Zr(1)–O(12)–C(13)	125.7 (7)
O(8)–Zr(1)–O(16)	150.09 (25)	Zr(2)–O(12)–C(13)	128.4 (7)
O(8)–Zr(1)–O(20)	100.8 (3)	Zr(1)–O(16)–C(17)	126.3 (7)
O(8)–Zr(1)–O(24)	99.2 (3)	Zr(1)–O(20)–C(21)	170.8 (10)
O(12)–Zr(1)–O(16)	82.33 (24)	Zr(1)–O(24)–C(25)	172.6 (11)
O(12)–Zr(1)–O(20)	163.5 (3)	Zr(2)–O(28)–C(29)	129.8 (7)
O(12)–Zr(1)–O(24)	96.5 (3)	Zr(2)–O(32)–C(33)	175.2 (8)
O(16)–Zr(1)–O(20)	99.0 (3)	Zr(2)–O(36)–C(37)	167.9 (9)
O(16)–Zr(1)–O(24)	99.4 (3)	Ba(3)–O(40)–Ba(3)	104.78 (23)
O(20)–Zr(1)–O(24)	99.5 (4)	Ba(3)–O(40)–C(41)	113.5 (10)
O(4)–Zr(2)–O(8)	72.28 (23)	Ba(3)′–O(40)–C(41)	141.5 (10)
O(4)–Zr(2)–O(12)	69.27 (22)		

The compound $[BaZr_2(O^iPr)_{10}]_2$ (**1**) is isolated as a colorless crystalline solid that is highly soluble in pentane and benzene. The solid melts at 278–280 °C. Room-temperature ^1H and $^{13}C\{^1H\}$ NMR data are consistent with C_{2v} molecular symmetry, indicating that the barium coordination to the $Zr_2(O^iPr)_9$ fragment observed in the solid-state structure (see below) is retained in solution.

The compound $Ba\{Zr_2(O^iPr)_9\}_2$ (**2**) is also a colorless crystalline solid, highly soluble in nonpolar solvents, although slightly less soluble than **1** in pentane. Crystals can be obtained at ambient temperature, as well as at −30 °C. Compound **2** does not melt reversibly but instead decomposes at 155 °C to yield compound **1** and $[Zr(O^iPr)_4]_n$. The occurrence of this decomposition was established upon an attempt to sublime **2** under high vacuum by using an infrared lamp. Only a viscous liquid condenses on the cold finger after several hours under these conditions. The ^1H NMR spectrum of this sublimate is identical with that obtained from an authentic[7] sample of $[Zr(O^iPr)_4]_n$ (obtained by heating the alcoholate, $Zr_2(O^iPr)_8(HO^iPr)_2$ under vacuum). The ^1H NMR spectrum of the residual solid left in the sublimation apparatus revealed only $[BaZr_2(O^iPr)_{10}]_2$ (**1**). This establishes the transformation of eq 1.

$$BaZr_4(O^iPr)_{18} \xrightarrow[\text{vacuum}]{\Delta} \tfrac{1}{2}[BaZr_2(O^iPr)_{10}]_2 + (2/n)[Zr(O^iPr)_4]_n \quad (1)$$

Both the ^1H and the ^{13}C NMR spectra of **2** are deceptively simple at room temperature, showing only one isopropyl environment. As the temperature is lowered, other resonances separate out, and at −60 °C the best resolved spectrum is obtained (although vicinal proton/proton couplings are not clearly resolved).

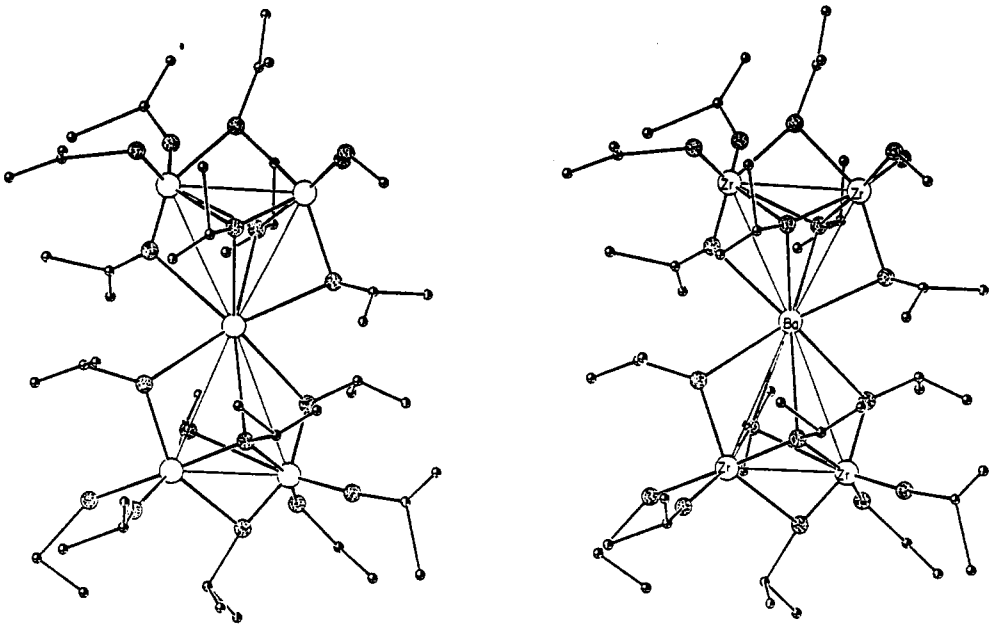

Figure 3. Stereo ORTEP drawing of the non-hydrogen atom of $BaZr_4(O^iPr)_{18}$. Oxygens are stippled, and several methyl carbons were not located. Lines between metals are not bonds but serve to identify the two triangular $BaZr_2$ subunits.

At −60 °C in the ^1H NMR spectrum there are two resonances in the methine region (δ 4.69 and δ 4.59), which integrate 1:2. The latter is clearly not a single septet. In the methyl region there are six resonances (δ 1.75, 1.71, 1.60, 1.59, 1.44, and 1.42), which integrate *approximately* 2:3:2:5:2:2. None of the methyl group resonances of **2** at −60 °C correspond to those of $[BaZr_2(O^iPr)_{10}]_2$ (**1**) nor those of $[Zr(O^iPr)_4]_n$. The observed methyl pattern is reminiscent of C_{2v} symmetry as displayed by **1**. The difference (i.e., one extra resonance) is probably due to the fact that there is indeed not C_{2v} symmetry in the solid-state structure of **2** (see below).

Solid-State Structure of $[BaZr_2(O^iPr)_{10}]_2$. The actual molecule (Figures 1 and 2) is a dimer of the simplest formula. A common structural unit for ligand-deficient compounds of metals favoring coordination number 6 is the M_3X_{11} triangle. In it, the anionic ligands occupy two μ_3-positions, three μ_2-positions (one on each edge of the triangle), and six terminal positions. Since "$BaZr_2(O^iPr)_{10}$" is deficient by one ligand from the M_3X_{11} stoichiometry, dimerization occurs at barium and the M_3X_{11} structural motif is achieved.

This heterobimetallic alkoxide can also be analyzed as a $Zr_2(O^iPr)_9^-$ face-shared bioctahedral unit binding to Ba^{2+} via two of its μ_2-O^iPr units and one terminal alkoxide from each zirconium. This is especially evident in Figure 1. This description of the structure is particularly useful, since Ba^{2+} is so much larger than Zr^{4+} (ionic radii 1.49 and 0.85 Å, respectively). As a result, all Ba–O distances are longer than all Zr–O distances. The Zr–O distances increase in the order Zr–O(terminal) = 1.931 Å < Zr–(μ-OBa) = 2.055 Å < Zr–(μ_2-OZr) = 2.199 Å < Zr–(μ_3-O) = 2.239 Å. The Ba–O distances increase in the order Ba–(μ-OBa) = 2.572 Å < Ba–(μ-OZr) = 2.748 Å < Ba–(μ_3-O) = 2.884 Å. The first two values indicate that zirconium-bound oxygens are weaker donors to barium than the oxygens that bridge two barium centers. Strong oxygen π-donation to Zr^{4+} is also indicated in the Zr–O–C(terminal) angles, which average 171.6°. The geometry at the oxygen that bridges two zirconium centers is planar (angles sum to 359.8°), but so is that at O(40), between the Ba^{2+} ions (angles sum to 359.8°). Ring-size contraints greatly distort the coordination geometry of barium from octahedral; this is evident in both Figures 1 and 2 and in the *trans*-O–Ba–O angles, which range from 114.55 to 167.63°.

Solid-State Structure of $BaZr_4(O^iPr)_{18}$. This compound gives large and well-formed single crystals, but a destructive phase transition occurs somewhere between 0 and 18 °C and has prevented collection of data at low temperature, where alkoxide structures are frequently better resolved crystallographically. Diffraction data that we were forced to collect at +18 °C have defined the $BaZr_4O_{18}$ substructure as that shown in Figure 3, but no suitable refinement model could be found for all the carbons. Since the $BaZr_4O_{18}$ core found is reasonable by all chemical criteria, as well as by comparison to that in $[BaZr_2(O^iPr)_{10}]_2$, we include this part of the structure here to completely define the chemical system studied (eq 1). Distances and angles are not reliable and are deposited only as supplementary material. The structure contains a "bow tie" or spiro Zr_2BaZr_2 unit, where barium is coordinated to two $Zr_2(O^iPr)_9^-$ units, to yield coordination number 8 for barium. The angle between the two $BaZr_2$ planes is 37°. A dihedral angle of 0 or 90° would eclipse the four oxygens from one $Zr_2(O^iPr)_9^-$ unit with respect to those of the second $Zr_2(O^iPr)_9^-$ unit. Thus, a value of 37° approaches the 45° dihedral angle that would give staggered conformation to the eight-coordinate polyhedron around barium.

Discussion

The structural types reported here have some precedent. The linking of two triangles by connection at an apex (cf. $[BaZr_2(O^iPr)_{10}]_2$) has been seen in $[(THF)NaGd_2Cp_2^*(THF)_2Cl_5]_2$, where THF on sodium bridges to the second sodium related by a center of symmetry.[9] The structure of $BaZr_4(O^iPr)_{18}$ is of the spiro class. This "bow-tie" form is seen in, e.g., $SnRe_4H_{14}(PR_3)_8$[10] and $SnFe_4(CO)_{16}$,[11] and is expected whenever a metal that prefers coordination number 2 or 4 is bound to two M_2 units.[11]

Synthetic control over the Ba:Zr ratio in the resulting heterometallic alkoxides is demonstrated here. This is an important factor in establishing targeted metal stoichiometries for oxide materials of interest.

A number of conclusions of importance to the theme of molecular precursors to solid materials follow from the results reported here. The loss of $[Zr(O^iPr)_4]_n$ by volatilization upon heating of $BaZr_4(O^iPr)_{18}$ exemplifies a limitation on heterometallic alkoxides as possible precursors for chemical vapor deposition: The very characteristics that promote desirable volatility of the heterometallic species also enable volatilization of lighter rearrangement substructures. Since it has been shown[7] that $[Zr(O^iPr)_4]_n$ has a degree of aggregation, n, of 3 or 4 in benzene, this loss of minimally a Zr_3 aggregate is *not* due to its existence as a structural subunit in the heterometallic precursor; significant

(9) Shen, Q.; Qi, M.; Lin, Y. *J. Organomet. Chem.* **1990**, *399*, 247.
(10) Westerberg, D. E.; Sutherland, B. R.; Huffman, J. C.; Caulton, K. G. *J. Am. Chem. Soc.* **1988**, *110*, 1642.
(11) Compton, N. A.; Errington, R. J.; Norman, N. C. *Adv. Organomet. Chem.* **1990**, *31*, 91.

rearrangement is involved in the transformation of eq 1.

The synthetic and structural principles of heterometallic alkoxide chemistry reported here should generalize to other large divalent cations such as lead or strontium as precursors for the zirconates of these metals. Additionally, while $BaZrO_3$ is cubic, the synthetic principles reported here should be useful in leading to ferroelectric $BaTiO_3$ and to antiferroelectric $PbZrO_3$.

Acknowledgment. This work was supported by the Department of Energy. We thank Scott Horn for skilled technical assistance.

Supplementary Material Available: For **1** and **2**, tables listing full crystallographic details, anisotropic thermal parameters, and bond distances and angles and a figure showing atom labeling (9 pages); tables of observed and calculated structure factors (21 pages). Ordering information is given on any current masthead page.

Contribution from the Department of Chemistry and Laboratory for Molecular Structure and Bonding, Texas A&M University, College Station, Texas 77843

Ring Opening of the $[Au(CH_2)_2PPh_2]_2X_4$ (X = Halogen) Metallacycle. Cleavage of Au^{III}–CH_2 Bonds

Raphael G. Raptis, John P. Fackler, Jr.,* John D. Basil, and Douglas S. Dudis

Received March 29, 1991

The reactions of $[Au(CH_2)_2PPh_2]_2$ (**1**) with excess ICl and Br_2 initially give the Au^{III} tetrahalide complexes $[Au(CH_2)_2PPh_2]_2X_4$ (X = Cl (**2**) or Br (**3**), respectively). Further reaction cleaves an Au^{III}–CH_2 bond to form the ring-opened dimers $Cl_3Au[\mu$-$(CH_2)_2PPh_2]AuCl_2(CH_2PPh_2CH_2I)$ (**4**) and $Br_3Au[\mu$-$(CH_2)_2PPh_2]AuBr_2(CH_2PPh_2CH_2Br)$ (**5**). Complexes **4** and **5** have been characterized by single-crystal X-ray crystallography: for **4**, monoclinic, $P2_1/n$, a = 10.322 (2) Å, b = 23.592 (4) Å, c = 15.516 (2) Å, β = 103.68 (1)°, V = 3671 (1) Å^3, Z = 4, refinement of 202 parameters with 2790 observed reflections gave R = 0.043 and R_w = 0.039; for **5**, monoclinic, $P2_1/n$, a = 10.392 (2) Å, b = 23.850 (5) Å, c = 15.964 (3) Å, β = 103.17 (2)°, V = 3853 Å^3, Z = 4, refinement of 211 parameters with 1668 observed reflections gave R = 0.058 and R_w = 0.055.

Introduction

The dimeric Au^I complex[1] $[Au(CH_2)_2PPh_2]_2$ (**1**) undergoes a two-[2] or four-electron[2h,3] oxidative-addition reaction to form Au^{II} or Au^{III} species, respectively. Dimers with both gold(III) centers containing halides in trans,[3] in cis,[4] or in one trans and one cis geometry[3b,c] have been characterized structurally (Chart I). Isomerization reactions[3b,4] between these various isomers have been observed.

The reaction of **1** with methylene halides gives[2d,e,5] μ-CH_2 "A-frame" products. The bridging ylide ligand $(CH_2)_2PPh_2^-$ does not appear to participate in this chemistry. It preserves the dimeric nature of the complexes by holding the two gold atoms in close proximity. The stability[6] of the Au–C bonds is enhanced by the presence of the ylide phosphonium center. The reaction chemistry of **1** is attributed to the proximity of the Au centers across the ylide ligand, which has a bite of ~3.0 Å. In the case of its Au^{III} derivatives, this Au···Au interaction causes a severe distortion of the geometry[7] of the d^8 metal atoms.

Three notable reactions have been observed in the chemistry of **1** and its derivatives wherein the ylide is an active component in the chemical processes. The reaction[8] of **1** with HCl (eq A of Scheme I) cleaves symmetrically two Au–CH_2 bonds thus breaking down the dimer into two monomeric Au^I–ylide fragments. The methyl phenyl analogue to **1**, $[Au(CH_2)_2PMePh]_2$, isomerizes[9] between its cis and trans geometrical forms (eq B), a process that cleaves and re-forms Au–CH_2 bonds. In polar solvents the Au^{II} complex $[Au(Ch_2)_2PPh_2]_2Cl_2$ disproportionates[10] (eq C) to a mixed-valence, Au^I/Au^{III} complex with one ylide ligand bridging the two gold atoms and the other chelating. In the case of the d^8 Au^{III} compounds of this ylide dimer system, the CH_2–Au σ bonds appear to be less labile. Reactions involving the cleavage of these Au–CH_2 bonds have not been described prior to this work.

In this paper we report that the Au^{III}–CH_2 bonds of the complexes $[Au(CH_2)_2PPh_2]_2X_4$, (X = Cl (**2**), Br (**3**)) can be cleaved by polar oxidizing agents or by prolonged reaction with halogens. The ring-opened dimeric complexes $Cl_3Au[\mu$-$(CH_2)_2PPh_2]$-$AuCl_2(CH_2PPh_2CH_2I)$ (**4**) and $Br_3Au[\mu$-$(CH_2)_2PPh_2]AuBr_2$-$(CH_2PPh_2CH_2Br)$ (**5**) have been characterized crystallographically.

Chart I

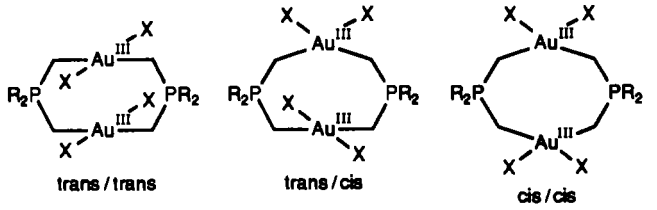

Scheme I

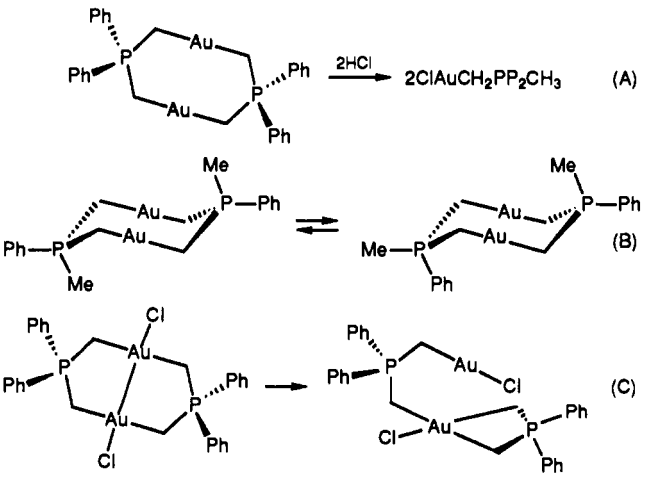

(1) (a) Cotton, F. A.; Wilkinson, G. *Advanced Inorganic Chemistry*, 5th ed.; John Wiley and Sons: New York, 1990; pp 949–950. (b) Basil, J. D.; Murray, H. H.; Fackler, J. P., Jr.; Tocher, J.; Mazany, A. M.; Trzcinscka-Bancroft, B.; Knachel, H.; Dudis, D.; Delord, T. J.; Marler, D. O. *J. Am. Chem. Soc.* **1985**, *107*, 6908. (c) Schmidbaur, H.; Mandl, J. R.; Frank, A.; Huttner, G. *Chem. Ber.* **1976**, *109*, 466–472. (d) See also: Jones, P. G. *Gold Bull.* **1981**, *14*, 159–166. Schmidbaur, H. *Angew. Chem., Intl. Ed. Engl.* **1983**, *22*, 907. Schmidbaur, H.; Hartman, C.; Rebev, G.; Müller, G. *Angew Chem., Intl. Ed. Engl.* **1987**, *26*, 1146.

*To whom correspondence should be addressed.

0020-1669/91/1330-3072$02.50/0